JCTC Journal of Chemical Theory and Computation

Understanding Rate Accelerations for Diels−Alder Reactions in Solution Using Enhanced QM/MM Methodology

Orlando Acevedo*,† and William L. Jorgensen*,‡

Department of Chemistry and Biochemistry, Auburn University, Auburn, Alabama 36849, and Department of Chemistry, Yale University, 225 Prospect Street, New Haven, Connecticut 06520-8107

Received March 30, 2007

Abstract: The Diels−Alder reactions of cyclopentadiene with 1,4-naphthoquinone, methyl vinyl ketone, and acrylonitrile have been investigated using QM/MM calculations in water, methanol, acetonitrile, and hexane. This extends an earlier AM1-based QM/MM study (*J. Phys. Chem. B* **2002**, *106*, 8078) that only investigated the reactions in water and utilized gas-phase optimized structures as starting points for computations of one-dimensional potentials of mean force (PMFs). Presently, the stationary points were located automatically in multiple solvents by computing two-dimensional PMFs, and the QM method is now PDDG/PM3. The resultant geometries are improved, and relative free energies of activation are well reproduced, e.g., $\Delta G^{\ddagger}$ for the reaction with naphthoquinone is computed to increase upon transfer from water to methanol, acetonitrile, and hexane by 3.2, 4.1, and 5.1 kcal/mol, while the experimental values are 3.4, 4.0, and 5.0 kcal/mol. Ab initio MP2/6-311+G(2d,p) calculations using the CPCM continuum solvent model on gas-phase CBS-QB3 geometries were also found to yield accurate $\Delta G^{\ddagger}$ values in water. However, only the QM/MM methodology reproduced the large rate increases in proceeding from aprotic solvents to water. The dominant factors for the rate variations are enhanced hydrogen bonding for the polarized transition states and reduction in hydrophobic surface area.

Introduction

The Diels−Alder reaction is one of the most powerful carbon−carbon bond forming processes and continues to be an important subject for both computational[1,2] and experimental studies.[3] Solvent effects on the reaction have received much attention due to striking rate accelerations that have been observed in aqueous solution.[4−11] However, not all Diels−Alder reactions benefit equally in water; e.g., the rate of the reaction between cyclopentadiene and 1,4-naphthoquinone is enhanced by up to 10 000-fold in aqueous over aprotic solvents,[9] while with acrylonitrile as the dienophile the acceleration is only 31-fold.[4] Reviews are available on the mechanistic aspects and solvent effects for Diels−Alder reactions,[3,7,12] and computational studies have clarified the microscopic variations in solvation along the reaction paths.[1,13−20] Early proposals that the primary factors responsible for the aqueous acceleration are reduction in hydrophobic surface area as the cycloaddition proceeds[4] and enhanced hydrogen bonding between water molecules and the transition state[13] are now largely accepted.[3−21]

To further explore the solvent-dependence of the reaction rates and geometries of the transition states at the atomic level, the Diels−Alder reactions between cyclopentadiene and three different dienophiles, 1,4-naphthoquinone, methyl vinyl ketone (MVK), and acrylonitrile (Scheme 1), have been investigated using the recently developed PDDG/PM3 semiemipirical molecular orbital method[22,23] in mixed quantum and molecular mechanics (QM/MM) simulations. In our prior QM/MM study of these reactions,[1] only water was

* Corresponding author e-mail: orlando.acevedo@auburn.edu (O.A.) and william.jorgensen@yale.edu (W.L.J.).
† Auburn University.
‡ Yale University.

10.1021/ct700078b CCC: $37.00
Published on Web 06/15/2007

Scheme 1. Diels−Alder Reactions between Cyclopentadiene and 1,4-Naphthoquinone, Methyl Vinyl Ketone, and Acrylonitrile

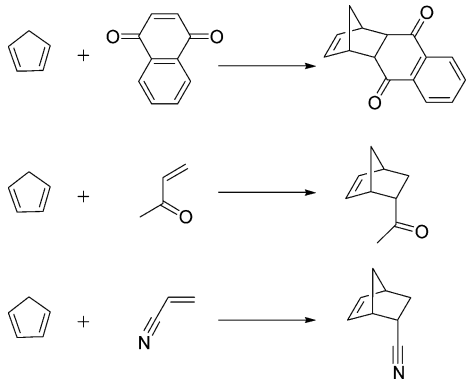

considered, and the QM/MM approach used AM1 as the QM method and relied on gas-phase optimized structures as starting points for computations of one-dimensional potentials of mean force (PMFs). In the current study, the reactants, transition structures, and cycloadducts have been located in a fully automated manner in up to four different solvents (water, methanol, acetonitrile, and hexane) using two-dimensional PMF calculations. Transition structures and activation barriers were computed with complete sampling of the geometry for the reacting systems and explicit representation of the solvent molecules. Problems with the use of one-dimensional PMF calculations, particularly for computed transition structures, are illustrated. In addition, changes in solvation along the reaction paths are fully characterized, and comparison is made with results of ab initio calculations with the CPCM solvation model.

Computational Methods

QM/MM calculations,[24] as implemented in BOSS 4.6,[25] were carried out with the reacting system treated using the semi-empirical PDDG/PM3 method. PDDG/PM3 has been extensively tested for gas-phase structures and energetics[22,23] and has given excellent results in solution-phase QM/MM studies for a variety of organic reactions.[26,27] The solvent molecules are represented with the TIP4P water model[28] and the united-atom OPLS force field for the nonaqueous solvents,[29] with the exception of hexane which used the all-atom version.[30] The systems consisted of the reactants, plus 390−395 solvent molecules for the nonaqueous solvents, or 730 molecules for water. The systems are periodic and tetragonal with $c/a = 1.5$; a is ca. 25, 27, 29, and 40 Å for water, methanol, acetonitrile, and hexane. To locate the minima and maxima on the free-energy surfaces, two-dimensional free-energy maps were constructed for each reaction using the lengths of the two forming CC bonds as the reaction coordinates (Figure 1). Free-energy perturbation (FEP) calculations were performed in conjunction with NPT Metropolis Monte Carlo (MC) simulations at 25 °C and 1 atm. The reactant state was defined by $R_{C1} = R_{C2} = 4.0$ Å, and the free-energy surfaces were flat in this vicinity.

In the present QM/MM implementation, the solute's intramolecular energy is treated quantum mechanically using PDDG/PM3; computation of the QM energy and atomic

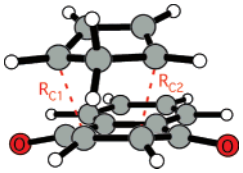

Figure 1. Reaction coordinates, R_{C1} and R_{C2}, for the Diels−Alder reaction between cyclopentadiene and 1,4-naphthoquinone. Illustrated structure is the transition structure from gas-phase PDDG/PM3 calculations ($R_{C1} = R_{C2} = 2.13$ Å).

charges is performed for each attempted move of the solute, which occurred every 100 configurations. For electrostatic contributions to the solute−solvent energy, CM3 charges[31] were obtained for the solute using PDDG/PM3 calculations with a scaling factor of 1.14. This is augmented with standard Lennard-Jones interactions between solute and solvent atoms using OPLS parameters.[30] This combination is appropriate for a PM3-based method as it minimizes errors in computed free energies of hydration.[32]

Solute−solvent and solvent−solvent intermolecular cutoff distances of 12 Å were employed based on all heavy atoms of the solute, the oxygens of water and methanol, the central carbon of acetonitrile, and carbon atoms of hexane. If any distance is within the cutoff, the entire solute−solvent or solvent−solvent interaction was included. Quadratic feathering of the intermolecular interactions within 0.5 Å of the cutoff was applied. Total translations and rotations were sampled in ranges that led to overall acceptance rates of about 41−47% for new configurations. FEP windows were run simultaneously on a Linux cluster at Yale and on computers located at the Alabama Supercomputer Center.

The complete basis set method CBS-QB3[33] was also used to characterize the transition structures and ground states in vacuum using Gaussian 03.[34] In a recent study, the CBS-QB3 method gave energetic results in the closest agreement to experiment for a set of 11 different pericyclic reactions compared to other ab initio and density functional theory methods.[35] The CBS-QB3 calculations were used for geometry optimizations and computations of vibrational frequencies, which confirmed all stationary points as either minima or transition structures and provided thermodynamic corrections. The effect of solvent was approximated by subsequent single-point calculations using the conductor-like polarizable continuum model (CPCM)[36] and the MP2/6-311+G(2d,p) theory level; default Gaussian 03 dielectric constants of 78.39, 32.63, 36.64, and 1.92 were used for water, methanol, acetonitrile, and hexane.

Results and Discussion

Structures. Geometries for the Diels−Alder reactions in solution were located with the QM/MM/MC calculations by starting from the gas-phase PDDG/PM3 cycloadduct structures and perturbing the two reacting carbon bonds between the diene and the dienophiles to find the transition structures (Figure 1). The endo addition mode was chosen in all cases, and for MVK, the *s*-cis conformation was used. These choices correspond to the preferred transition state from ab initio calculations[37] as well as experimental stereoselective preferences.[6,11] All internal degrees of freedom other than

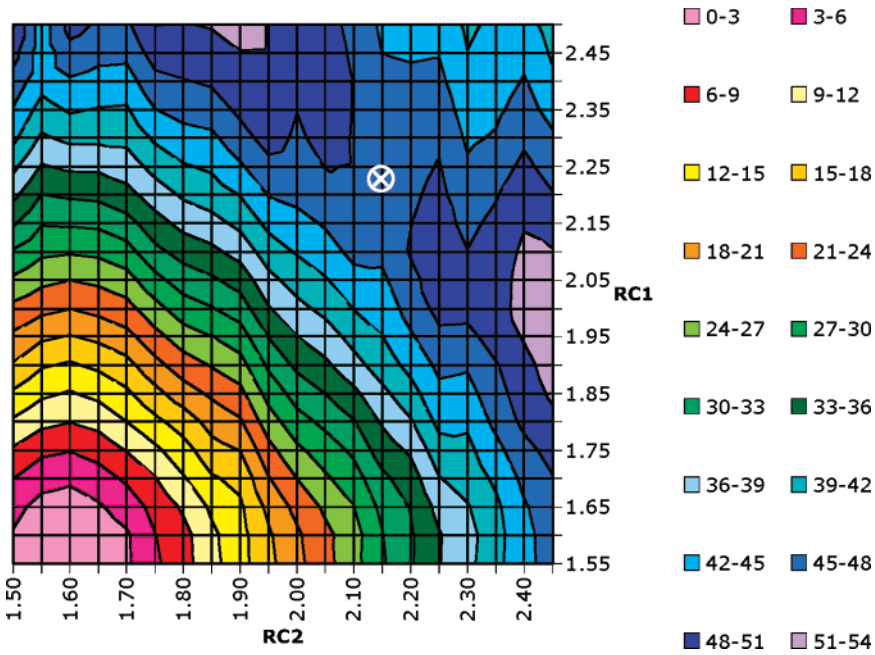

Figure 2. Two-dimensional potential of mean force (free-energy map) for the Diels−Alder reaction between cyclopentadiene and 1,4-naphthoquinone in hexane; ⊗ marks the saddle point that represents the solution-phase transition structure. All distances are in Å, and relative free energy is in kcal/mol.

the two reaction coordinates R_{C1} and R_{C2} were fully sampled during the simulations. The initial ranges for R_{C1} and R_{C2} were 1.5−2.5 Å. Each FEP calculation entailed 5 million (M) configurations of equilibration and 10 M configurations of averaging and was computed using increments of 0.05 Å. As an example, the resultant map for the Diels−Alder reaction between cyclopentadiene and 1,4-naphthoquinone in hexane is shown in Figure 2. To locate the critical points more precisely, the regions surrounding the cycloadduct and transition state from the initial maps were explored in increments of 0.01 Å.

The previous one-dimensional PMF approach required a number of intermediate geometries connecting the transition structure to the reactants and cycloadduct for use as initial geometries in the QM/MM simulations.[1] The geometries were derived by following the intrinsic reaction coordinate with ab initio calculations and by interpolation. A single reaction coordinate was defined between two dummy atoms located at the midpoint of the reacting carbons in the diene and dienophile; however, this approach provides uncertainty in locating the transition structures. To illustrate the problem, one-dimensional PMF calculations were performed here with three different choices for the reaction coordinate (Figure 3); these calculations used PDDG/PM3, 0.01 Å increments, 5−10 M configurations of equilibration, and 10−30 M configurations of averaging for each FEP window. Without the ab initio reference points, the predicted transition structures are found to be highly dependent on the chosen reaction coordinate. Similar results were found for all three Diels−Alder reactions in Scheme 1. The current 2-D approach, in contrast, does not require the ab initio calculations and effectively samples all geometries including the transition structure. The geometrical results for the transition structures from the 2-D QM/MM/FEP maps are listed in Table 1 along with the gas-phase CBS-QB3 findings.

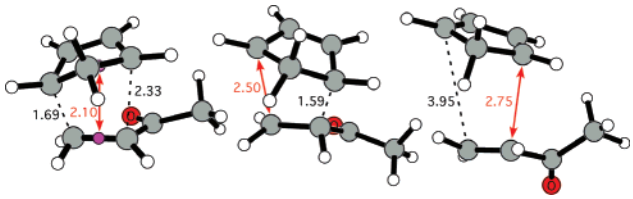

Figure 3. Transition-state geometries for the Diels−Alder reaction between cyclopentadiene and methyl vinyl ketone in water from one-dimensional potential of mean force calculations using three choices for the reaction coordinates (colored in red). All distances are in Å.

The PDDG/PM3 and CBS-QB3 results for the cyclopentadiene plus 1,4-naphthoquinone transition structure in the gas phase are notably similar and reflect a symmetrical, synchronous process. The two bond lengths remain essentially the same in solution, though they are lengthened by about 0.1 Å from the gas-phase values. The asynchronicity Δr is close to the level of uncertainty in the results, ca. ±0.02 Å. Since the bond-lengthening is similar in all solvents, it can be attributed to the thermal averaging and location of the variational transition state in solution (free-energy saddle-point) as opposed to the conventional transition state from the gas-phase potential energy calculations. The degree of asynchronicity in vacuum and solution becomes significant for the reactions with the unsymmetrical dienophiles, MVK and acrylonitrile. For the gas-phase reactions, the PDDG/PM3 method yields Δr values of ca. 0.1 Å, which underestimates the CBS-QB3 results of 0.6 and 0.4 Å. The latter values are similar to prior results, and the ordering is consistent with the greater capacity for resonance stabilization of negative charge by a keto group than a cyano group. In both cases the computed asynchronicity from the PDDG/PM3-based QM/MM simulations increases in water and methanol to ca. 0.3 Å, while Δr is predicted to be 0.18 Å

Table 1. Computed Bond Lengths (Å) and Asynchronicity ($\Delta r = R_{C2} - R_{C1}$) for the Transition Structures of the Diels−Alder Reactions with Cyclopentadiene at 25 °C and 1 Atm

	gas[a]	CBS-QB3[b]	water[c]	CH_3OH[c]	CH_3CN[c]	hexane[c]
1,4-naphthoquinone						
R_{C1}	2.13	2.18	2.22	2.18	2.25	2.22
R_{C2}	2.13	2.17	2.25	2.21	2.19	2.19
Δr	0.0	−0.01	0.03	0.03	−0.06	−0.03
methyl vinyl ketone						
R_{C1}[d]	2.08	1.99	2.01	2.02	2.06	
R_{C2}	2.18	2.60	2.34	2.28	2.24	
Δr	0.10	0.61	0.33	0.26	0.18	
acrylonitrile						
R_{C1}[d]	2.09	2.05	2.00	2.01		
R_{C2}	2.18	2.45	2.28	2.28		
Δr	0.09	0.40	0.28	0.27		

[a] PDDG/PM3 optimizations. [b] Gas-phase optimizations. [c] From the QM/MM/FEP free-energy maps using PDDG/PM3. [d] Shorter distance is with the terminal carbon of the dienophile.

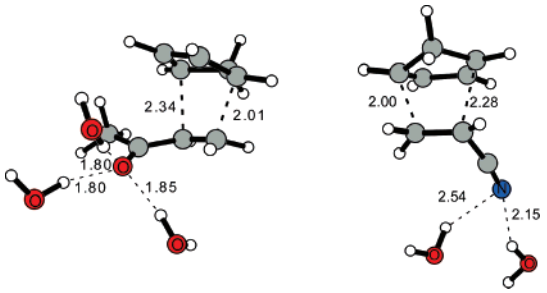

Figure 4. Typical snapshots of transition structures for the reactions between cyclopentadiene and methyl vinyl ketone and acrylonitrile in water from the QM/MM/MC simulations. Only water molecules nearest the carbonyl or cyano group are illustrated; distances are in Å.

for the reaction with MVK in the dipolar aprotic solvent acetonitrile. As discussed previously, the greater asynchronicity in the protic solvents can be attributed to enhanced hydrogen bonding at the oxygen of MVK and nitrogen of acrylonitrile in the transition states.[1,13,16] Typical structures at the transition states from the simulations of these two reactions in water are provided in Figure 4. The number of hydrogen-bonded water molecules increases from two for acrylonitrile to three for methyl vinyl ketone. The hydrogen bonds are also shorter and stronger to the keto oxygen than cyano nitrogen. The hydrogen-bond lengths agree well with results of previous ab initio calculations on the same systems complexed to a single water molecule.[16] The changes in solvation are discussed further below.

Energetics. The computed activation barriers for the Diels−Alder reactions are summarized in Tables 2 and 3. Uncertainties for the free energies are calculated by propagating the standard deviation (σ_i) on each individual ΔG_i. Free energy changes were obtained with statistical uncertainties of only 0.008−0.03 kcal/mol in each window; this implies overall uncertainties in the computed values for $\Delta G^{\ddagger}$ and ΔG_{rxn} of 0.5 and 0.6 kcal/mol, respectively.

Similar to previous QM/MM results for Diels−Alder reactions,[1,27] the relative free energies of activation are in good agreement with experiment, while the absolute values are overestimated by 10−15 kcal/mol (Tables 2 and 3). As discussed previously,[1] the accuracy of the absolute free energies is adversely affected by several issues. First, the entropy of the reactants is underestimated owing to incomplete sampling and the need for a cratic entropy correction. The latter is small, ca. 3 cal/mol·K, and stems from constraining the reactants to a sphere of 4.0 Å radius with 1 M standard states. A small rate reduction can also be expected from dynamical effects or solvent friction.[19]

Table 2. Free Energy Changes, ΔG (kcal/mol), at 25 °C for the Diels−Alder Reactions between Cyclopentadiene and the Three Dienophiles Using PDDG/PM3/MM/MC

	water	CH_3OH	CH_3CN	hexane
1,4-naphthoquinone				
$\Delta G^{\ddagger}$ (calc)	26.0	29.2	30.1	31.1
$\Delta G^{\ddagger}$ (exptl)[a]	16.6	20.0[b]	20.6	21.6
ΔG_{rxn} (calc)	−20.1	−17.7	−17.2	−15.4
$\Delta G^{\ddagger}_{retro}$ (calc)	46.0	46.8	47.3	46.4
methyl vinyl ketone				
$\Delta G^{\ddagger}$ (calc)	32.2	36.4	35.7	
$\Delta G^{\ddagger}$ (exptl)[a]	19.2	21.6[b]	22.6	
ΔG_{rxn} (calc)	−25.8	−19.3	−19.4	
$\Delta G^{\ddagger}_{retro}$ (calc)	58.0	55.7	55.1	
acrylonitrile				
$\Delta G^{\ddagger}$ (calc)	34.0	35.2		
$\Delta G^{\ddagger}$ (exptl)[c]	22.2	23.8		
ΔG_{rxn} (calc)	−16.7	−15.6		
$\Delta G^{\ddagger}_{retro}$ (calc)	50.7	50.9		

[a] Reference 9. [b] In ethanol. [c] Reference 4; 30 °C.

Table 3. Free Energy of Activation, $\Delta\Delta G^{\ddagger}$ (kcal/mol), at 25 °C Relative to Water for the Diels−Alder Reactions Using PDDG/PM3/MM/MC

	water	CH_3OH	CH_3CN	hexane
1,4-naphthoquinone				
$\Delta\Delta G^{\ddagger}$ (calc)	0.0	3.2	4.1	5.1
$\Delta\Delta G^{\ddagger}$ (exptl)[a]	0.0	3.4[b]	4.0	5.0
methyl vinyl ketone				
$\Delta\Delta G^{\ddagger}$ (calc)	0.0	4.2	3.5	
$\Delta\Delta G^{\ddagger}$ (exptl)[a]	0.0	2.4[b]	3.4	
acrylonitrile				
$\Delta\Delta G^{\ddagger}$ (calc)	0.0	1.2		
$\Delta\Delta G^{\ddagger}$ (exptl)[c]	0.0	1.6		

[a] Reference 9. [b] In ethanol. [c] Reference 4; 30 °C.

However, the largest contribution to the overestimation of the activation barriers lies in the quantum mechanics methodology. PDDG/PM3 calculations yield gas-phase activation enthalpies of 34.8, 33.4, and 33.0 kcal/mol for the reactions of cyclopentadiene with naphthoquinone, methyl vinyl ketone, and acrylonitrile, respectively. The prior AM1 calculations yielded similar results, 31.0, 30.1, and 29.8 kcal/mol, while the experimental values are in the 10−20 kcal/mol range.[1] The use of more intensive QM calculations does not guarantee better accuracy. For example, the gas-phase activation barrier for the cyclopentadiene plus MVK reaction has been computed to be in the range of 2−35 kcal/mol for a variety of ab initio and density functional methods; the experimental $\Delta H^{\ddagger}$ is 12.8 kcal/mol in isooctane.[1,9,37] For reasonable quantitative accuracy for the absolute activation barriers, MP3/6-31G(d), B3LYP/6-31G(d), or higher levels are required. Unfortunately, the use of such ab initio or DFT methods in the current QM/MM approach is impractical in view of the system sizes and need for thorough configurational sampling in the fluid simulations. While the overestimated activation energy barrier for MVK in methanol (Table 3) came primarily from semiempirical QM error, part of the deviation was due to a higher noise level in the Monte Carlo simulations; a reduction of sampling in exchange for an ab initio method would likely increase the noise level further offsetting any accuracy gained from using a high-level QM method. For the previous QM/MM/MC calculations of one-dimensional free-energy profiles, ca. 3.5 million single-point QM calculations were required per profile.[1] The present computations of two-dimensional free-energy surfaces increase the demands to ca. 50 million QM calculations per map. Though there is clearly room for improvement in the semiempirical QM methods, it is notable that the present QM/MM/MC methodology reproduces well the observed rate acceleration in water over methanol and aprotic solvents (Table 3) and provides gas-phase geometries which compare favorably to CBS-QB3 results (Table 1).

Continuum Solvent Models. Previous theoretical work on the Diels−Alder reaction explored implicit solvent models to describe the effects of hydration.[15,17,20] For example, Cativiela et al. used the self-consistent reaction-field (SCRF) continuum approach coupled with the PM3 semiempirical method to model the reaction between cyclopentadiene and methyl vinyl ketone and found the exo *s*-trans conformation to be the most stable transition structure.[17] This appears to be an artifact of PM3 as the exo *s*-trans transition structure is the least stable of the four endo/exo and *s*-cis/*s*-trans options at the MP3/6-31G(d) level.[37] In fact, AM1, PM3, and PDDG/PM3 all yield very similar results for the energetics of the four transition structures, as summarized in the Supporting Information (Table S1). It may also be noted that an abnormally short H−H distance predicted by PM3 between a methylene hydrogen on cyclopentadiene and a hydrogen from methyl vinyl ketone in the exo *s*-trans TS is corrected with PDDG/PM3 (Supporting Information Figure S2). The problem can be traced to the PM3 core repulsion formula (CRF), which incorrectly describes H−H nonbonded interactions in the 1.7−1.8 Å range.[22]

Table 4. MP2/6-311+G(2d,p)/CPCM Results for $\Delta G^{\ddagger}$ (kcal/mol) at 25 °C for the Diels−Alder Reactions with Cyclopentadiene[a]

	water	CH_3OH	CH_3CN	hexane
1,4-naphthoquinone				
$\Delta G^{\ddagger}$ (calc)	16.7	17.9	16.5	18.4
$\Delta G^{\ddagger}$ (exptl)[b]	16.6	20.0[d]	20.6	21.6
methyl vinyl ketone				
$\Delta G^{\ddagger}$ (calc)	19.5	20.9	19.6	
$\Delta G^{\ddagger}$ (exptl)[b]	19.2	21.6[d]	22.6	
acrylonitrile				
$\Delta G^{\ddagger}$ (calc)	22.1	23.5		
$\Delta G^{\ddagger}$ (exptl)[c]	22.2	23.8		

[a] CPCM single point on CBS-QB3 optimized geometries. [b] Reference 9. [c] Reference 4; 30 °C. [d] In ethanol.

The use of the conductor-like polarizable continuum model (CPCM) in conjunction with ab initio single-point energy calculations has been shown to provide good accuracy for computing free energies of hydration for a variety of organic molecules and ions.[38] To explore the accuracy of CPCM for the present systems, single-point energy calculations at the MP2/6-311+G(2d,p) level were carried out on the gas-phase CBS-QB3 geometries. The absolute $\Delta G^{\ddagger}$ values computed with this MP2/CPCM approach are in excellent agreement with the experimental values in water (Table 4). However, the continuum model significantly underestimates the effects of switching from water as the solvent to methanol or acetonitrile. Specific changes in hydrogen bonding are expected to be important along the reaction path, and they are not reflected in the continuum treatment. In addition, differences in the structures of the transition states due to solvation (Table 1) are not taken into account when using the gas-phase geometries, though this is expected to be a secondary issue and apparently did not adversely effect the CPCM results for water. However, for acetonitrile and water, the CPCM approach yields nearly identical activation barriers for the cyclopentadiene plus 1,4-naphthoquinone, 16.5 and 16.7 kcal/mol, while the experimental difference is 4.0 kcal/mol.[9] A similar pattern is seen for the cyclopentadiene plus MVK reaction (Table 4). The QM/MM/MC calculations with their explicit representation of the solvent molecules overcome this limitation (Table 3).

Solvent Effects. The QM/MM/MC simulations capture the key contributions of the medium effects as evidenced by the good agreement between the computed and observed changes in the free energies of activation (Table 3). In water, hydrophobicity-promoted aggregation of diene and dienophile certainly contributes to the lowering of activation barriers for Diels−Alder reactions.[4−10] The burial of surface area is relatively constant, and the associated rate enhancement is steady at about a factor 10.[1,13] The key contributor to larger rate increases in protic solvents is preferential stabilization of the transition structures through enhanced hydrogen bonding.[1,13,14] The present results are fully consistent with these ideas. As an example, the solute−solvent energy pair distributions for the reaction between cyclopentadiene and 1,4-naphthoquinone in water and hexane are presented in Figure 5. The interaction energies are quantified by analyzing the QM/MM/MC results in three representative

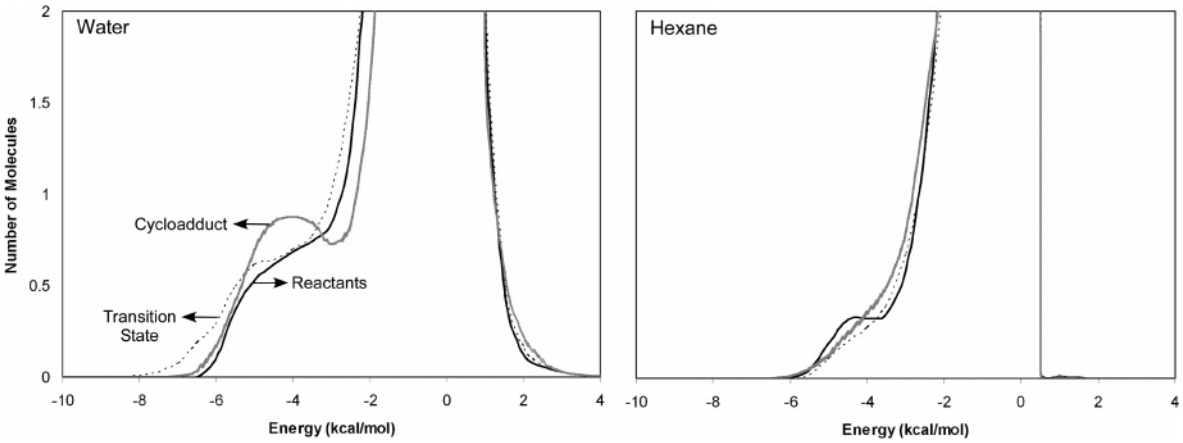

Figure 5. Solute−solvent energy pair distributions for the Diels−Alder reaction between cyclopentadiene and 1,4-naphthoquinone for the reactants, transition state, and cycloadduct in water and hexane at 25 °C. The ordinate records the number of solvent molecules that interact with the solutes and their interaction energy on the abscissa. Units for ordinate are number of molecules per kcal/mol.

FEP windows, near the reactants, transition structure, and cycloadducts. The distributions record the average number of water or hexane molecules that interact with the reacting system and their corresponding energies. Hydrogen bonding between the solute and solvent is found in the left-most region with the most attractive interaction energies. The large bands near 0 kcal/mol is the result of the many solvent molecules located in the outer shells. The critical difference in water is the extension of the distribution for the transition state to low energy. The hydrogen bonding is similar for the reactant and product as they both have keto groups; however, the hydrogen bonds become stronger for the transition state owing to diene to dienophile charge transfer and concomitant enhanced C^+O^- polarization of the carbonyl groups.[13,16] Consistent with the previous QM/MM simulations,[1] it is also found that the number of solute-water hydrogen bonds increases by about one in going from the reactant to TS in water. If the curves in Figure 5 are integrated to a cutoff energy of −4.0 kcal/mol, the number of water molecules is 2.3, 3.0, and 3.0 for the reactant, TS, and product. If the integration is extended to −3.5 kcal/mol, the corresponding values are 3.1, 3.8, and 3.9.

The solute−solvent structure for the Diels−Alder reactions in water can be further characterized by radial distribution functions, $g(R)$. Hydrogen bonding between the oxygens of naphthoquinone and methyl vinyl ketone and the hydrogens of water, O(dienophile)−H(water), should yield contacts shorter than ca. 2.5 Å. The corresponding $g_{OH}(R)$ gives the probability of finding a hydrogen of water at a distance R from oxygens of the dienophile. Accordingly, both Diels−Alder reactions show a well-defined first peak centered around 1.9 Å with minima near 2.5 Å that reflects the hydrogen bonds (Figure 6). In both cases, the hydrogen bonding is clearly greatest for the transition state. Integration of the first peaks to the minima near 2.5 Å reveals averages of 3.0 hydrogen bonds between the dienophile oxygens and water molecules for the transition states in both cases. This is well illustrated in Figure 4 for the MVK transition state, while in the Supporting Information, Figure S1, a snapshot for the naphthoquinone transition state illustrates a configuration with two hydrogen bonds for each carbonyl oxygen.

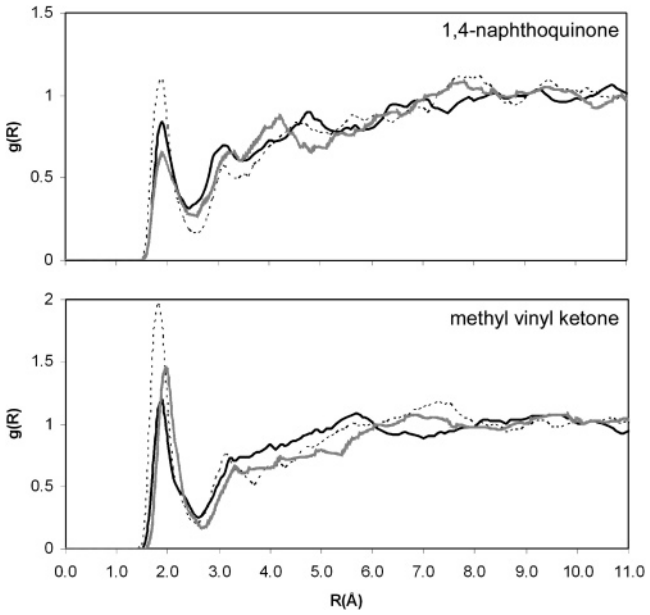

Figure 6. Computed O(dienophile)−H(water) radial distribution functions for the reactions of cyclopentadiene with 1,4-naphthoquinone and methyl vinyl ketone: reactants (solid black curve), transition state (dashed curve), and cycloadduct (solid gray curve) at 25 °C.

The hydrogen bonds are a little longer on average for the naphthoquinone case as reflected in Figures 4, 6, and S1.

Conclusion

QM/MM/MC simulations have been carried out for three Diels−Alder reactions in water, methanol, acetonitrile, and hexane yielding good accord between the computed and observed variations in the free energies of activation. In an advance over the prior related study,[1] two-dimensional free energy surfaces were computed as a function of the lengths of the two forming bonds in a fully automated manner. This avoids potential artifacts and uncertainty in location of transition states associated with the use of single reaction coordinates. The present results also confirm the general view that rate accelerations for such Diels−Alder reactions in

protic solvents arise primarily from enhanced hydrogen-bonding to hydrogen-bond accepting groups in the dienophile. Ab initio MP2/CPCM calculations were also carried out to examine the solvent effects on reaction rates. Excellent results were obtained for the reactions in water; however, the substantial rate enhancements over the aprotic solvents were not reproduced by the continuum methodology. Clearly, a QM/MM/MC approach with the QM at the ca. MP2/6-311+G(d,p) level is most desirable but difficult to achieve with the present level of MC sampling that is required to give acceptable precision for the free-energy surfaces.

Acknowledgment. Gratitude is expressed to the National Science Foundation (CHE-0446920) and the Alabama Supercomputer Center for support of this research.

Supporting Information Available: Illustration of the naphthoquinone transition state in water, a comparison of PM3 and PDDG/PM3 transition structures for the MVK reaction, and a table with gas-phase activation energies for the MVK reaction. This material is available free of charge via the Internet at http://pubs.acs.org.

References

(1) Chandrasekhar, J.; Shariffskul, S.; Jorgensen, W. L. *J. Phys. Chem. B* **2002**, *106*, 8078−8085.

(2) (a) Acevedo, O.; Evanseck, J. D. *Org. Lett.* **2003**, *5*, 649−652. (b) DeChancie, J.; Acevedo, O.; Evanseck, J. D. *J. Am. Chem. Soc.* **2004**, *126*, 6043−6047. (c) Guimarães, C. R. W.; Udier-Blagovic, M.; Jorgensen, W. L. *J. Am. Chem. Soc.* **2005**, *127*, 3577−3588. (d) Pieniazek, S. N.; Houk, K. N. *Angew. Chem., Int. Ed.* **2006**, *45*, 1442−1445.

(3) (a) Corey, E. J. *Angew. Chem., Int. Ed.* **2002**, *41*, 1650−1667. (b) Nicolaou, K. C.; Snyder, S. A.; Montagnon, T.; Vassilikogiannakis, G. *Angew. Chem., Int. Ed.* **2002**, *41*, 1668−1698.

(4) Rideout, D. C.; Breslow, R. *J. Am. Chem. Soc.* **1980**, *102*, 7816−7817.

(5) (a) Breslow, R.; Maitra, U.; Rideout, D. *Tetrahedron Lett.* **1983**, *24*, 1901−1904. (b) Breslow, R.; Guo, T. *J. Am. Chem. Soc.* **1988**, *110*, 5613−5617. (c) Breslow, R. *Acc. Chem. Res.* **1991**, *24*, 159−164. (d) Sarma, D.; Pawar, S. S.; Deshpande, S. S.; Kumar, A. *Tetrahedron Lett.* **2006**, *47*, 3957−3958.

(6) Breslow, R.; Maitra, U. *Tetrahedron Lett.* **1984**, *25*, 1239−1240.

(7) (a) Breslow, R.; Rizzo, C. J. *J. Am. Chem. Soc.* **1991**, *113*, 4340−4341. (b) Blokzijl, W.; Blandamer, M. J.; Engberts, J. B. F. N. *J. Am. Chem. Soc.* **1991**, *113*, 4241−4246. (c) Blokzijl, W.; Engberts, J. B. F. N. *J. Am. Chem. Soc.* **1992**, *114*, 5440−5442. (d) Blokzijl, W.; Engberts, J. B. F. N. In *Structure and Reactivity in Aqueous Solution*; Cramer, C. J., Truhlar, D. G., Eds.; American Chemical Society: Washington, DC, 1994; Vol. 568, pp 303−317. (e) Breslow, R.; Zhu, Z. *J. Am. Chem. Soc.* **1995**, *117*, 9923−9924. (f) Breslow, R.; Connors, R.; Zhu, Z. *Pure Appl. Chem.* **1996**, *68*, 1527−1533. (g) Otto, S.; Bertoncin, F.; Engberts, J. B. F. N. *J. Am. Chem. Soc.* **1996**, *118*, 7702−7707. (h) Wijnen, J. W.; Zavarise, S.; Engberts, J. B. F. N.; Charton, M. *J. Org. Chem.* **1996**, *61*, 2001−2005. (i) Otto, S.; Engberts, J.; Kwak, J. C. T. *J. Am. Chem. Soc.* **1998**, *120*, 9517−9525. (j) Otto, S.; Boccaletti, G.; Engberts, J. B. F. N. *J. Am. Chem. Soc.* **1998**, *120*, 4238−4239. (k) van Mersbergen, D.; Wijnen, J. W.; Engberts, J. B. F. N. *J. Org. Chem.* **1998**, *63*, 8801−8805. (l) Otto, S.; Engberts, J. B. F. N. *J. Am. Chem. Soc.* **1999**, *121*, 6798−6806. (m) Otto, S.; Engberts, J. B. F. N. *Pure Appl. Chem.* **2000**, *72*, 1365−1372. (n) Rispens, T.; Engberts, J. B. F. N. *Org. Lett.* **2001**, *3*, 941−943. (o) Schreiner, P. R. *Chem. Soc. Rev.* **2003**, *32*, 289−296. (p) Wittkopp, A.; Schreiner, P. R. *Chem. Eur. J.* **2003**, *9*, 407−414. (q) Breslow, R. *Acc. Chem. Res.* **2004**, *37*, 471−478. (r) Rispens, T.; Engberts, J. B. F. N. *J. Phys. Org. Chem.* **2005**, *18*, 725−736. (s) Tiwari, S.; Kumar, A. *Angew. Chem., Int. Ed.* **2006**, *45*, 4824−4825. (t) Kleiner, C. M.; Schreiner, P. R. *Chem. Commun.* **2006**, 4315−4317.

(8) (a) Otto, S.; Blokzijl, W.; Engberts, J. B. F. N. *J. Org. Chem.* **1994**, *59*, 5372−5376. (b) van der Wel, G. K.; Wijnen, J. W.; Engberts, J. B. F. N. *J. Org. Chem.* **1996**, *61*, 9001−9005.

(9) Engberts, J. B. F. N. *Pure Appl. Chem.* **1995**, *67*, 823−828.

(10) Wijnen, J. W.; Engberts, J. B. F. N. *J. Org. Chem.* **1997**, *62*, 2039−2044.

(11) Cativiela, C.; García, J. I.; Gil, J.; Martínez, R. M.; Mayoral, J. A.; Salvatella, L.; Urieta, J. S.; Mainar, A. M.; Abraham, M. H. *J. Chem. Soc., Perkin Trans.* **1997**, *2*, 653−660.

(12) (a) Sauer, J.; Sustmann, R. *Angew. Chem., Int. Ed.* **1980**, *19*, 779−807. (b) Cativiela, C.; García, J. I.; Mayoral, J. A.; Salvatella, L. *Chem. Soc. Rev.* **1996**, *25*, 209−218. (c) Wittkopp, A.; Schreiner, P. R. In *The chemistry of dienes and polyenes*; Rappoport, Z., Ed.; Wiley: New York, 2000; Vol. 2, pp 1029−1088.

(13) Blake, J. F.; Jorgensen, W. L. *J. Am. Chem. Soc.* **1991**, *113*, 7430−7432.

(14) (a) Cativiela, C.; García, J. I.; Mayoral, J. A.; Avenoza, A.; Peregrina, J. M.; Roy, M. A. *J. Phys. Org. Chem.* **1991**, *4*, 48−52. (b) Cativiela, C.; García, J. I.; Mayoral, J. A.; Royo, A. J.; Salvatella, L.; Assfeld, X.; Ruiz-lopez, M. F. *J. Phys. Org. Chem.* **1992**, *5*, 230−238. (c) Jorgensen, W. L.; Blake, J. F.; Lim, D.; Severance, D. L. *J. Chem. Soc., Faraday Trans.* **1994**, *90*, 1727−1732. (d) Harano, Y.; Sato, H.; Hirata, F. *J. Am. Chem. Soc.* **2000**, *122*, 2289−2293.

(15) Ruiz-López, M. F.; Assfeld, X.; García, J. I.; Mayoral, J. A.; Salvatella, L. *J. Am. Chem. Soc.* **1993**, *115*, 8780−8787.

(16) Blake, J. F.; Lim, D.; Jorgensen, W. L. *J. Org. Chem.* **1994**, *59*, 803−805.

(17) Cativiela, C.; Dillet, V.; García, J. I.; Mayoral, J. A.; Ruiz-López, M. F.; Salvatella, L. *J. Mol. Struct. (THEOCHEM)* **1995**, *331*, 37−50.

(18) Furlani, T. R.; Gao, J. *J. Org. Chem.* **1996**, *61*, 5492−5497.

(19) (a) Pak, Y.; Voth, G. A. *J. Phys. Chem. A* **1999**, *103*, 925−931. (b) Hu, H.; Kobrak, M. N.; Xu, C.; Hammes-Schiffer, S. *J. Phys. Chem. A* **2000**, *104*, 8058−8066.

(20) Kong, S.; Evanseck, J. D. *J. Am. Chem. Soc.* **2000**, *122*, 10418−10427.

(21) Blokzijl, W.; Engberts, J. B. F. N. *Angew. Chem., Int. Ed. Engl.* **1993**, *32*, 1545−1579.

(22) Repasky, M. P.; Chandrasekhar, J.; Jorgensen, W. L. *J. Comput. Chem.* **2002**, *23*, 1601−1622.

(23) (a) Tubert-Brohman, I.; Guimarães, C. R. W.; Repasky, M. P.; Jorgensen, W. L. *J. Comput. Chem.* **2003**, *25*, 138−150. (b) Tubert-Brohman, I.; Guimarães, C. R. W.; Jorgensen, W. L. *J. Chem. Theory Comput.* **2005**, *1*, 817−823.

(24) (a) Aqvist, J.; Warshel, A. *Chem. Rev.* **1993**, *93*, 2523−2544. (b) Gao, J. *Acc. Chem. Res.* **1996**, *29*, 298−305. (c) Kaminski, G. A.; Jorgensen, W. L. *J. Phys. Chem. B* **1998**, *102*, 1787−1796.

(25) Jorgensen, W. L.; Tirado-Rives, J. *J. Comput. Chem.* **2005**, *26*, 1689−1700.

(26) (a) Acevedo, O.; Jorgensen, W. L. *Org. Lett.* **2004**, *6*, 2881−2884. (b) Acevedo, O.; Jorgensen, W. L. *J. Am. Chem. Soc.* **2005**, *127*, 8829−8834. (c) Acevedo, O.; Jorgensen, W. L. *J. Am. Chem. Soc.* **2006**, *128*, 6141−6146. (d) Acevedo, O.; Jorgensen, W. L. *J. Org. Chem.* **2006**, *71*, 4896−4902.

(27) Acevedo, O.; Jorgensen, W. L.; Evanseck, J. D. *J. Chem. Theory Comput.* **2007**, *3*, 132−138.

(28) Jorgensen, W. L.; Chandrasekhar, J.; Madura, J. D.; Impey, W.; Klein, M. L. *J. Chem. Phys.* **1983**, *79*, 926−935.

(29) (a) Jorgensen, W. L. *J. Phys. Chem.* **1986**, *90*, 1276−1284. (b) Jorgensen, W. L.; Briggs, J. M. *Mol. Phys.* **1988**, *63*, 547−558. (c) Jorgensen, W. L.; Briggs, J. M.; Contreras, M. L. *J. Phys. Chem.* **1990**, *94*, 1683−1686. (d) Briggs, J. M.; Matsui, T.; Jorgensen, W. L. *J. Comput. Chem.* **1990**, *11*, 958−971.

(30) (a) Jorgensen, W. L.; Maxwell, D. S.; Tirado-Rives, J. *J. Am. Chem. Soc.* **1996**, *118*, 11225−11236. (b) Price, M. L.; Ostrovsky, D.; Jorgensen, W. L. *J. Comput. Chem.* **2001**, *22*, 1340−1352. (c) Thomas, L. L.; Christakis, T. J.; Jorgensen, W. L. *J. Phys. Chem. B* **2006**, *100*, 21198−21204.

(31) Thompson, J. D.; Cramer, C. J.; Truhlar, D. G. *J. Comput. Chem.* **2003**, *24*, 1291−1304.

(32) Udier-Blagovic, M.; De Tirado, P. M.; Pearlman, S. A.; Jorgensen, W. L. *J. Comput. Chem.* **2004**, *25*, 1322−1332.

(33) Ochterski, J. W.; Petersson, G. A.; Montgomery, J. A. *J. Chem. Phys.* **1996**, *104*, 2598−2619.

(34) Frisch, M. J.; Trucks, G. W.; Schlegel, H. B.; Scuseria, G. E.; Robb, M. A.; Cheeseman, J. R.; Montgomery, J. A., Jr.; Vreven, T.; Kudin, K. N.; Burant, J. C.; Millam, J. M.; Iyengar, S. S.; Tomasi, J.; Barone, V.; Mennucci, B.; Cossi, M.; Scalmani, G.; Rega, N.; Petersson, G. A.; Nakatsuji, H.; Hada, M.; Ehara, M.; Toyota, K.; Fukuda, R.; Hasegawa, J.; Ishida, M.; Nakajima, T.; Honda, Y.; Kitao, O.; Nakai, H.; Klene, M.; Li, X.; Knox, J. E.; Hratchian, H. P.; Cross, J. B.; Bakken, V.; Adamo, C.; Jaramillo, J.; Gomperts, R.; Stratmann, R. E.; Yazyev, O.; Austin, A. J.; Cammi, R.; Pomelli, C.; Ochterski, J. W.; Ayala, P. Y.; Morokuma, K.; Voth, G. A.; Salvador, P.; Dannenberg, J. J.; Zakrzewski, V. G.; Dapprich, S.; Daniels, A. D.; Strain, M. C.; Farkas, O.; Malick, D. K.; Rabuck, A. D.; Raghavachari, K.; Foresman, J. B.; Ortiz, J. V.; Cui, Q.; Baboul, A. G.; Clifford, S.; Cioslowski, J.; Stefanov, B. B.; Liu, G.; Liashenko, A.; Piskorz, P.; Komaromi, I.; Martin, R. L.; Fox, D. J.; Keith, T.; Al-Laham, M. A.; Peng, C. Y.; Nanayakkara, A.; Challacombe, M.; Gill, P. M. W.; Johnson, B.; Chen, W.; Wong, M. W.; Gonzalez, C.; Pople, J. A. *Gaussian 03, revision D.01*; Gaussian, Inc.: Wallingford, CT, 2004.

(35) Guner, V.; Khuong, K. S.; Leach, A. G.; Lee, P. S.; Bartberger, M. D.; Houk, K. N. *J. Phys. Chem. A* **2003**, *107*, 11445−11459.

(36) Cossi, M.; Rega, N.; Scalmani, G.; Barone, V. *J. Comput. Chem.* **2003**, *24*, 669−681.

(37) Jorgensen, W. L.; Lim, D.; Blake, J. F. *J. Am. Chem. Soc.* **1993**, *115*, 2936−2942.

(38) Takano, Y.; Houk, K. N. *J. Chem. Theory Comput.* **2005**, *1*, 70−77.

CT700078B